Environmental Engineering and Management Journal

July 2015, Vol.14, No. 7, 1735-1742
http://omicron.ch.tuiasi.ro/EEMJ/

"Gheorghe Asachi" Technical University of Iasi, Romania

PHYSICAL-MECHANICAL PROPERTIES OF NEW GREEN BUILDING MATERIALS BASED ON GLASS WASTE

Rosa Taurino[1]*, Fernanda Andreola[1], Cristina Leonelli[1], Tiziano Manfredini[1], Paolo Gastaldi[2], Luisa Barbieri[1]

[1]Università degli Studi di Modena e Reggio Emilia, Dipartimento di Ingegneria "Enzo Ferrari", 10 via Vivarelli, 41125 Modena, Italy
[2]Intals Spa, 3 Viale Lombardia, 27020, Parona (PV), Italy

Abstract

Recently several innovative suggestions on how industrial wastes can be utilised in new products have been presented in literature, e.g. as filler or additives in concrete, incorporated in ceramic materials to produce glass-ceramics and pavement construction. In this work, metallurgical materials from secondary aluminium scrap processing and glass waste derived from treatments of packaging and fluorescent lamps were considered for fabrication of new ceramic materials using powder technology and sintering process.
The effect of composition and heat treatment temperature, on the sintering process and then final properties, were evaluated. The results showed that, with the proper firing temperature, lightweight ceramic materials containing high amount of glass waste and an innovative product resulting from the processing of secondary aluminum (ArgAlum®) can be produced. The low water absorption (< 1%), low density (< 2 g/cm^3) and the good flexural strength (16-20 MPa) associated to relatively low sintering temperatures obtained with the addition of ArgAlum®-can be considered as promising initial results to obtain new green building materials.

Key words: by-product, ceramic material, low density materials, glass recycling, waste

Received: December, 2014; Revised final: June, 2015; Accepted: June, 2015

1. Introduction

Waste material, defined as any type of material by-product of human and industrial activity, could contribute to increased sustainability of industrial operations by conserving virgin materials and increasing the sustainable use of resources. Categories of waste that the new EC Waste Framework Directive 2008/98/EC (WFD) has recognized as candidate for "end-of-waste" (EoW) criteria can include the waste streams of construction and demolition waste, ashes, slags, scrap metals, aggregates, tyres, textiles, compost, paper and glass (Watkins et al., 2013; Szőke et al., 2014; Li et al., 2014). Three different alternative raw materials can be considered as substituted of traditional ones for the ceramic and building material industries: the glass waste from containers (GWC), glass from fluorescent lamps and products from secondary aluminum scraps processing.

According to data reported by CoReVe, the Italian Consortium for the collection, recycling and reuse of waste from packaging glass in Italy, in 2013 approximately 2,186,300 tons of packaging glass have been put on the market in Italy and the 73% of that it has been collected by separate collection. In other words, around 1,596,000 tons of the packaging glass are recovered mainly (99%) in glassworks and 1% in alternative recovery processes (ceramic industry, building, others glass sectors) (Co.Re.Ve., 2014; Andreola et al., 2013).

* Author to whom all correspondence should be addressed: e-mail: rosa.taurino@unimore.it; Phone: +39 0592056230; Fax: +39 0592056243

Fluorescent lamps are widely world-wide used due to their long life and energy saving capability. A typical fluorescent lamp is composed by a glass tube coated with different blends of metallic and rare-earth phosphor salts with electrodes located at both ends of the tube (Jansma, 2003). Light tubes are generally made by a soft sodium–calcium glass whereas the materials at the ends, which are connected to the light cap, are made of hard glass with higher lead content. These lamps contain mercury (Hg) as a source of fluorescent radiation, cadmium (Cd) and lead (Pb). Hence, their untreated disposal causes serious health and pollution problems (Andreola et al., 2010)

This work evaluates the potential use of these glass wastes with a product from secondary aluminum process, in the production of new ceramic materials for building sector. The secondary aluminium industry generates a salt-cake waste currently disposed of in a conventional landfill. As much as 50% of the content of this waste is mixed salt (sodium and potassium chlorides). In addition, black dross that is not economical to reprocess in a rotary furnace for aluminium recovery ends up in landfills (Gil, 2005; Gil and Korili, 2010; Wöhlk et al., 1987; Tociu et al., 2014). The composition of the dross is similar to that of salt cake, except that it contains higher concentrations of metallic aluminium (up to 20%) and correspondingly lower amounts of salts. Because of the high solubility of the salts in water, these residues, when put in landfills, represent a potential source of pollution surface-water and groundwater supplies (Tsakiridis, 2012).

Nevertheless, a methodology for salt cake waste from secondary aluminum dross recovery was patented by Intals S.p.A. (Gastaldi and Vedani, 2008). This technique maximizes aluminum recovery, and it also produces a new material, coded, as ArgAlum®, constituted of corundum (Al_2O_3), as main crystalline phase. Specifically, ArgAlum® is an innovative product, with registered trade mark since 24.01.2008 in Class 6 “Common metals and alloys; materials for metal constructions; metallic transportable constructions; metallic materials for railways; non-electric metallic cables and wires; ironmongery, small metal hardware; safes; metal products not included in other classes; raw minerals”. It is an eco-friendly material which drastically reduces the need for virgin raw materials mainly in the production of Portland cement and alumina cement with low environmental impact, bricks and brick materials, expanded clay, mineral fibres for thermal insulation (rock wool). ArgAlum® is an inorganic mineral material made from a mixture of oxides, with the appearance of dark sand with a grain size of max 1 mm, sold on the national and international market for almost 10 years.

ArgAlum® contains no substances of very high concern (SVHC) contemplated in the ECHA (European Chemicals Agency) “Candidate List of Substances of Very High Concern for Authorisation” in concentrations over 0.1% in weight (Candiadate List of substances of very high concern for Authorisation). Registering EPD – Environmental Product Declaration - is a further step towards recognising the quality, innovation and sustainability for ArgAlum® (more on PRODUCT INFORMATION data sheet).

The purpose of this work was to test both the compatibility of ArgAlum® with the two different kinds of glass wastes above described and the influence of their different chemical composition on the technological and of processing parameters. The aim was to prepare new green building product based totally on recovery raw material in replacement of traditional feldspar and quartz sand.

2. Experimental procedure

2.1. Materials

In this study glass waste derived from glass containers and fluorescence lamps were chosen. These two wastes were used with refractory clay: K kaolin ceramic grade (Balco, Italy).

In Table 1 is reported the chemical composition of the glass wastes. The highest amount of alkaline oxide, in particular Na_2O combined with the lower amount of silica in the fluorescent lamp composition, underline a higher fluxing action and sintering temperature decrease of fluorescent lamp with respect to packaging glass.

Table 1. Chemical composition of glass wastes

Oxide	***Fluorescence lamp glass waste (wt%)***	***Glass container Waste (wt%)***
SiO_2	68.0	71.7
Al_2O_3	2.27	2.25
Na_2O	17.5	12.5
K_2O	1.59	1.0
MgO	2.96	2.0
CaO	5.1	9.5
SrO	0.07	-
BaO	0.94	-
PbO	0.77	-
Fe_2O_3	0.08	0.43
Sb_2O_3	0.08	-
TiO_2	0.002	0.07
P_2O_5	0.05	-

In Table 2 is reported the chemical composition of ArgAlum®, consisting of corundum (Al_2O_3), quartz (SiO_2), aluminium (Al) and spinel ($MgAl_2O_4$) as main crystalline phases and NaCl.

Table 2. Chemical composition of Argalum

Oxide/element	***wt%***
Al_2O_3	60-80%
Al	1-6%
SiO_2	5-11%
FeO	1-3%
MgO	3-7%
Cl	<0.5%

A series of ceramic batches containing 80 wt% of glass and 20 wt% of a refractory clay were prepared (labeled 80_V20_C for the sample with glass container and $80_{Vfl}20_C$ with fluorescence lamp glass).

In order to investigate the effect of ArgAlum® (Ar) on physical mechanical properties of these new ceramic materials for building sector, a different concentration of Ar was added to the batch replacing glass and/or clay. Thus $X_VY_CXY_A$ composition have been obtained, where X is a digit denoting the concentration of glass, Y the concentration of the clay and moreover XY the presence of Ar in replacement of glass or clay. The list of the prepared samples are reported in Table 3, the batch chemical compositions are completely different with respect to the traditional ceramic products, traditional tiling ceramics, building bricks and roof tiles (EN 14411, 2006).

In order to prepare suitable press-powder, the raw materials were ground and sieved below 500 μm. Each batch composition was prepared by dry-grinding, humidified with 6 wt% of distilled water, and finally the green samples were uniaxial pressed at 40 MPa. Bar samples (50 mm ×5 mm ×4 mm) were sintered in an electric laboratory furnace (Nambertherm) at 10°C/min heating and 1 h soaking step at different temperatures (950-1000-1050-1100°C range). Moreover, parallelepiped samples (100 mm×8 mm×8 mm) were uniaxial pressed at 40 MPa and the obtained specimens were used for flexural strength.

2.2. Characterization of samples

For the fired samples, measurements of linear shrinkage (LS %) and water absorption (WA %) according to ISO 10545-3 were performed. Total porosity (P_T), was evaluated by the difference between absolute density, ρ_{ab} and apparent density, ρ_a, of ceramics (Eq. 1). Apparent density was estimated by a dry flow Pycnometer (Micromeritics GeoPyc 1360) using bulk sample of 1 cm^2 of area, while ρ_{ab} by He displacement Pycnometer (Micromeritics ACCUPYC 1330), after crashing and milling the samples below 45 μm.

$$P\ (\%) = 100\ x\ \rho_{ab} - \rho_d/\rho_{ab} \quad (1)$$

A series of five samples of each composition was used for the evaluation of flexural tests performed according to UNI EN ISO 178. The maximum flexural strength at break (σ_b) and the maximum deformation (ε_{max}) were evaluated for at least five specimens. The microstructure of the fired materials was analyzed by scanning electron microscope (ESEM Quanta 200, FEI Company, USA).

Table 3. List of the prepared samples, including composition and temperature treatment

Sample	*Glass container (wt%)*	*Fluorescence lamp glass (wt%)*	*Clay (wt%)*	*ArgAlum® (wt%)*	*Temperature (°C)*
80_V20_{C950}	80	-	20	0	950
80_V20_{C1000}	80	-	20	0	1000
80_V20_{C1050}	80	-	20	0	1050
80_V20_{C1100}	80	-	20	0	1100
$80_V10_C10_{A950}$	80	-	10	10	950
$80_V10_C10_{A1000}$	80	-	10	10	1000
$80_V10_C10_{A1050}$	80	-	10	10	1050
$80_V10_C10_{A1100}$	80	-	10	10	1100
$70_V20_C10_{A950}$	70	-	20	10	950
$70_V20_C10_{A1000}$	70	-	20	10	1000
$70_V20_C10_{A1050}$	70	-	20	10	1050
$70_V20_C10_{A1100}$	70	-	20	10	1100
$80_{Vfl}20_{C850}$	-	80	20	-	850
$80_{Vfl}20_{C900}$	-	80	20	-	900
$80_{Vfl}20_{C950}$	-	80	20	-	950
$80_{Vfl}20_{C1000}$	-	80	20	-	1000
$80_{Vfl}20_{C1050}$	-	80	20	-	1050
$80_{Vfl}20_{C1100}$	-	80	20	-	1100
$80_{Vfl}10_C10_{A950}$	-	80	10	10	950
$80_{Vfl}10_C10_{A1000}$	-	80	10	10	1000
$80_{Vfl}10_C10_{A1050}$	-	80	10	10	1050
$80_{Vfl}10_C10_{A1100}$	-	80	10	10	1100
$70_{Vfl}20_C10_{A950}$	-	70	20	10	950
$70_{Vfl}20_C10_{A1000}$	-	70	20	10	1000
$70_{Vfl}20_C10_{A1050}$	-	70	20	10	1050
$70_{Vfl}20_C10_{A1100}$	-	70	20	10	1100

The effect of ArgAlum® on the sample color was determined by performing color measurements on both samples before and after the addition of Argalum, by a spectrophotometer (SP60) using the CIELAB method. The method defines a color through three parameters, L^*, a^*, and b^*, measuring brightness, red/green, and yellow/blue color intensities, respectively (Johnston, 1973). The method allows, moreover, to define a color difference as ΔE^*, based on the relationship (2), where ΔL^*, Δa^*, and Δb^* measure the differences in luminosity and in chromaticity between two colors.

$$\Delta E^* = [(\Delta L^*)^2+(\Delta a^*)^2+(\Delta b^*)^2]^{1/2} \quad (2)$$

In this way, the variations due to the addition of ArgAlum® were determined.

3. Results and discussion

3.1. Physical properties of final ceramics

Fig. 1 presents the firing shrinkage and water absorption of the ceramic bodies made with 80% of glass waste and 20% of clay. The $80_{Vfl}20_C$ sample shows higher shrinkage at low temperature, which can be attributed to the high Na_2O content in the fluorescence glass waste.

In fact, the alkaline oxide rich glass waste, by acting as a fluxing agent, contributed to a decrease of the thermal treatment of about 100°C as can be seen in Fig. 1.

Moreover, a water absorption values within 8-8.3% occurs at 900°C and 1000°C for $80_{Vfl}20_C$ and 80_V20_C mixtures respectively.

The sintering behavior changed after the addition of ArgAlum® as confirmed by Figs. 2 and 4. It is evident from Fig. 2a a decreasing trend in the firing shrinkage with Argalum addition at lower firing temperatures (950-1000°C). This was confirmed by the porosity evaluation. The maximum porosity percentage of 28.97% is observed for $80_V10_C10_{A1000}$, compared to 21.77% for 80_V20_{C1050} sample (Table 5).

In all of the case, the decrease of linear shrinkage, at lower temperature, could be ascribed to the decreased sintering activity of samples due to the addition of corundum, the main crystalline phase of ArgAlum®. As a consequence of the decreasing of the densification, the water absorption values increase.

Interesting and better results were obtained for the sample $70_V20_C10_{A1050}$: 1) minor linear shrinkage, 2) minor water absorption, 3) minor apparent density (Table 5), which may be attributed to the expansion phenomena.

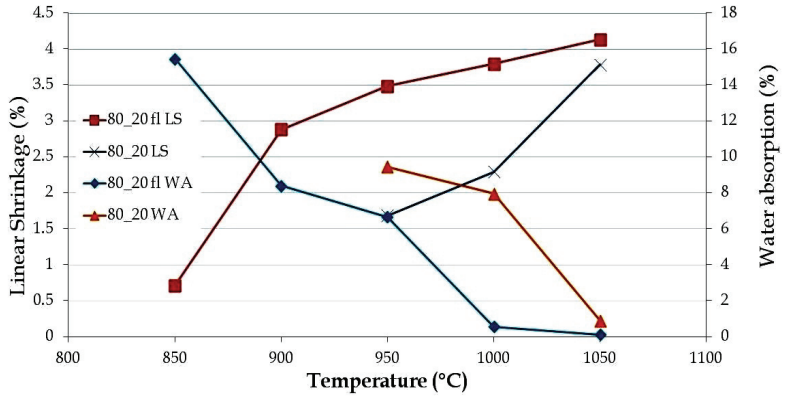

Fig. 1. Linear shrinkage and water absorption of ceramic batch 80_V20_C and $80_{Vfl}20_C$ fired at various temperatures

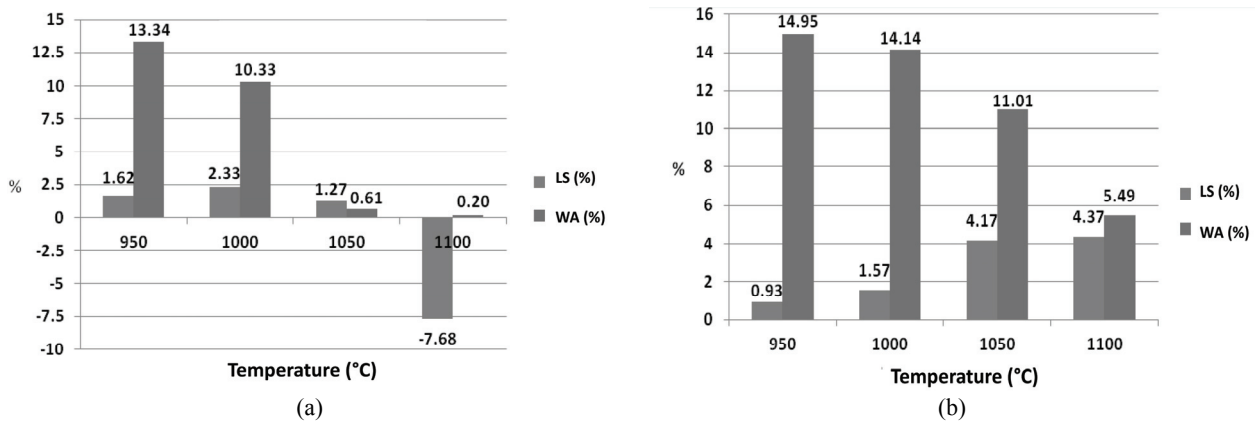

(a) (b)

Fig. 2. Linear shrinkage and water absorption values of sample (a) $80_V10_C10_A$ and (b) $70_V20_C10_A$

The low apparent density and water absorption indicate that closed porosity was formed and that vetrification took place. Fig. 3 reports the image of the sample before and after adding of ArgAlum®. At higher temperature (1100°C) starts overfiring, with WA near 7.16% and about 9.68% of linear expansion. The $80_{Vfl}20c$ composition shows similar behaviour, in agreement with the content of Ar.

As can be seen in Fig 4, in agreement with the content of Ar, the $80_{Vfl}20c$ composition also shows a decreasing trend in the firing shrinkage. Because of the diminution of the densification, the water absorption values increase. The results related to samples obtained at 1100°C are not reported because the samples melt and became deformed at higher temperatures. In addition, in this case, interesting results have been obtained for one composition, the $70_V20_C10_{A1050}$ sample. The addition of ArgAlum® in the mixture with fluorescence lamp glass leads of a decrease in density and water absorption at low thermal temperature resulting advantageous for obtaining porous materials with low water absorption.

Apparent density and total porosity values are listed in Table 5. It can be observed that density ranges from 1.83 g/cm^3 to a minimum of 0.68 g/cm^3 for samples with higher porosity values, while the absolute densities of the these ceramics increase from 2.48 to 2.57 g/cm^3 with ArgAlum®. The absolute densities of these materials are similar to those of the traditional glass-ceramics materials (2.56 g/cm^3), while the apparent density values are lower than those usually measured on some traditional ceramics such as floor (Manfredini and Pellacani, 1992).

Concerning the colour of sintered samples, reported in Table 4, it is pale brown for the 80v20c composition and became green at higher temperature. Finally, the colour of $80_V10_C10_A$ and $70_{Vfl}20_C10_A$ strongly points to grey, due to the presence of metallic aluminum in the Ar powders.

3.2. Structure and mechanical properties of final ceramics

SEM images, taken on the cross section of the fired samples, are reported in Fig. 5a-d. SEM observations confirmed the results of LS% and porosity evaluation and highlight that the microstructure varies with the Ar addition and temperature treatment. It must be observed that sample produced by sintering 80v20c composition at 1000°C shows the presence of distinct grains (Fig. 5a), while the specimen prepared at higher temperature 1050°C (Fig. 5b, 5d) shows the presence of a vitreous phase which is evident in several zones where the microstructure is not perfectly visible since polycrystalline grains are covered by a layer of glass produced by the liquid phase present at high temperature during the sintering process.

The specimen prepared at higher temperature have great amount of heterogeneous porosity that contribute to the decrease of density. The flexural strength, a property that strongly depends on the porosity and microstructural defects of specimen (Alonso-Santurde et al., 2012), has been measured only for some samples, the more interesting for future applications. The flexural strength varied from 4.8 MPa to 28.93 MPa for the composition 80_V20_C, the highest value was obtained for sample 80_V20_{C1050}.

(a) **(b)** **(c)**

Fig. 3. Images of sample (a) $80v20c_{1050}$, (b) $80_V10_C10_{A1050}$ and (c) $70_V20_C10_{1100}$

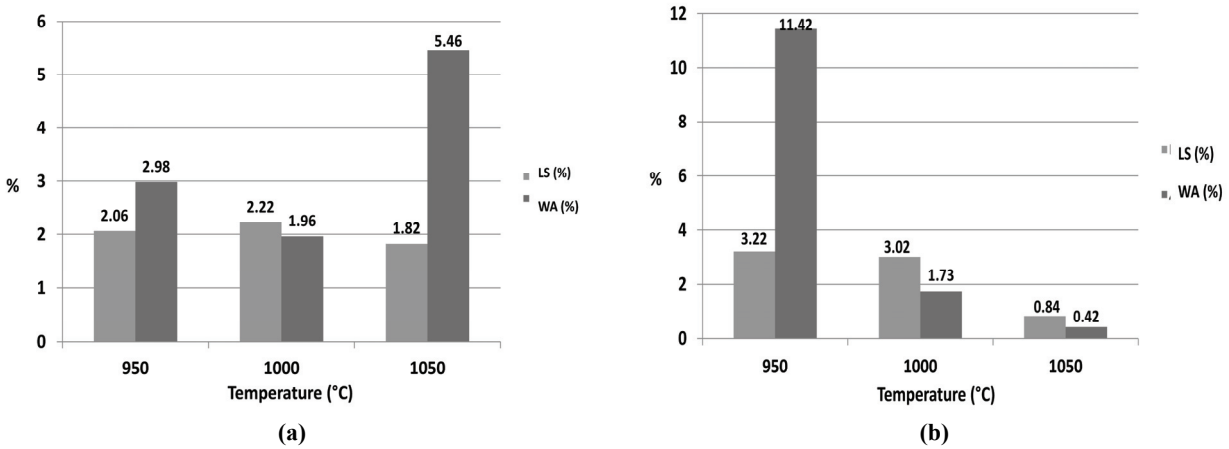

(a) **(b)**

Fig. 4. Linear shrinkage and water absorption values of sample a) $80_{Vfl}10_C10_A$ and b) $70_{Vfl}20_C10_A$

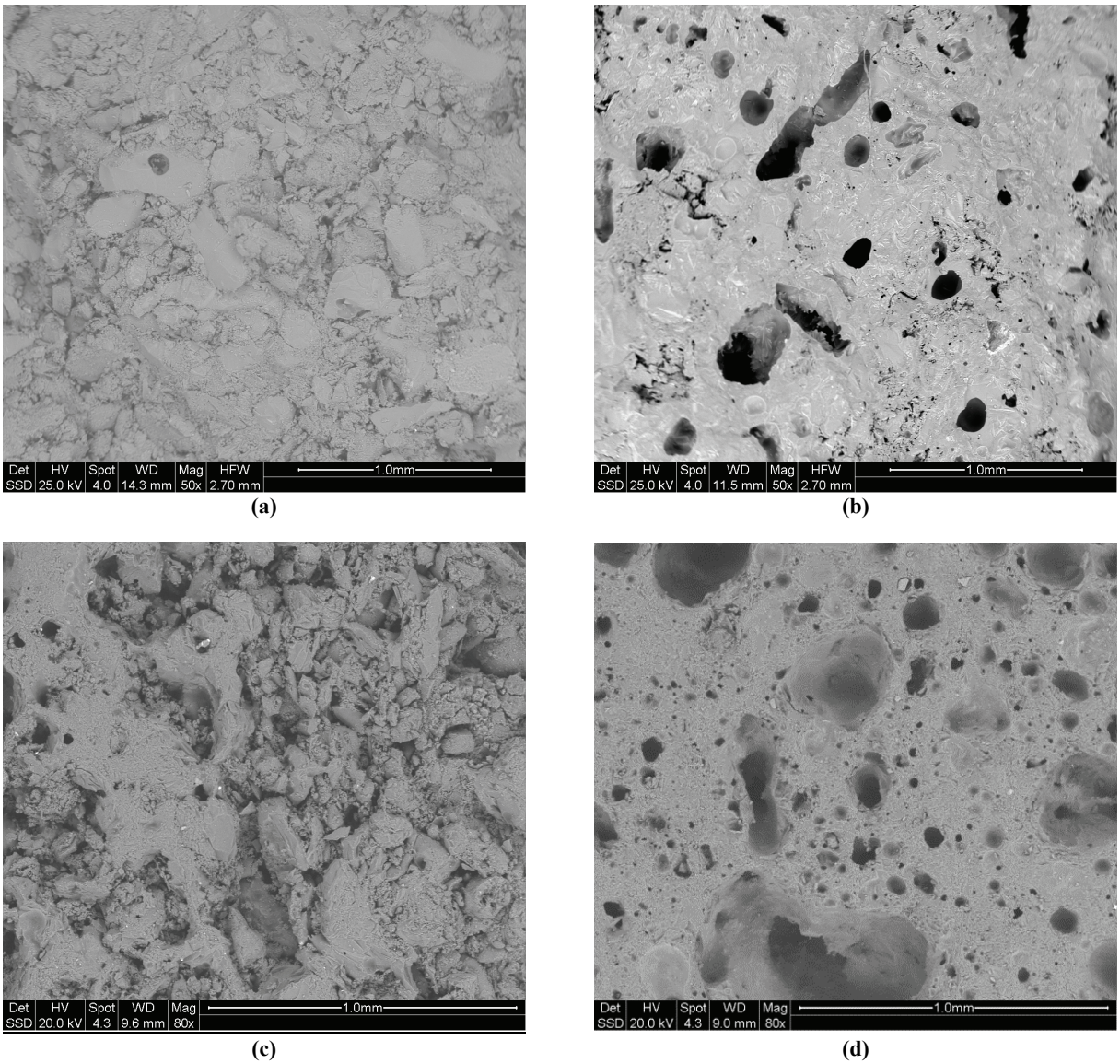

Fig. 5. SEM micrographs of sample a) $80_V20_{C1000,}$ b) $80_V20_{C1050,}$ c) $80_V10_C10_{A1000}$, d) $80_V10_C10_{A1050}$

Table 4. Colorimetric measurements

Sample	***L***	***a***	***b***	***ΔE***
80_V20_{C950}	80.38±0.45	2.8±0.13	13.53±0.51	-
80_V20_{C1000}	78.86±0.65	1.69±0.14	13.60±0.35	-
80_V20_{C1050}	67.16±0.84	-1.90±0.22	12.80±0.31	-
$80_V10_C10_{A950}$	75.84±0.55	0.92±0.06	8.51±0.19	7.07
$80_V10_C10_{A1000}$	67.37±0.57	-0.08±0.28	7,76±0,26	12.04
$80_V10_C10_{A1050}$	65.25±0.22	-0.92±0.13	6.35±0.11	7.29
$70_V20_C10_{A950}$	81.09±0.16	0.79±0.04	6.23±0.11	5.27
$70_V20_C10_{A1000}$	80.61±0.21	0.68±0.04	5.77±0.12	6.00
$70_V20_C10_{A1050}$	76.47±0.65	0.32±0.06	5.53±0.25	7.39
$80_{Vfl}20_{C950}$	76.82±0.98	5.63±0.19	12.55±0.41	-
$80_{Vfl}20_{C1000}$	63.06±0.47	5.15±0.20	11.33±0.32	-
$80_{Vfl}20_{C1050}$	60.66±0.44	1.83±0.15	6.93±0.08	-
$80_{Vfl}10_C10_{A950}$	58.24±0.97	1.47±0.18	3.84±0.24	6.98
$80_{Vfl}10_C10_{A1000}$	62.79±1.19	1.27±0.07	4.25±0.23	8.08
$80_{Vfl}10_C10_{A1050}$	60.42±1.36	0.53±0.07	3.62±0.17	3.56
$70_{Vfl}20_C10_{A950}$	53.88±0.71	0.88±0.17	2.95±0.24	24.49
$70_{Vfl}20_C10_{A1000}$	61.98±0.55	1.51±0.09	5.69±0.27	6.80
$70_{Vfl}20_C10_{A1050}$	56.68±1.49	0.24±0.13	3.21±0.32	11.43

Table 5. Physical and mechanical characteristics: apparent density (ρ_{ap}), total porosity (P_T), maximum flexural strength at break (σ_b) and the maximum deformation (ε_{max})

Sample	ρ_{ap} *(g/cm^3)*	P_T *(%)*	σ_b *(MPa)*	ε_{max} *(%)*
80_V20_{C950}	2.07	16.53	4.8±1.34	0.435±0.001
80_V20_{C1000}	1.94	21.77	9.95±2.59	0.022±0.012
80_V20_{C1050}	2.02	18.55	28.93±2.79	0.016±0.015
$80_V10_C10_{A950}$	1.79	28.97	2.73±0.82	0.045±0.005
$80_V10_C10_{A1000}$	1.79	28.97	9.94±3.43	0.022±0.010
$80_V10_C10_{A1050}$	1.47	41.67	13.82±1.47	0.022±0.020
$80_V10_C10_{A1100}$	0.95	62.30	-	-
$70_V20_C10_{A950}$	1.82	27.77	2.07±0.69	0.023±0.004
$70_V20_C10_{A1000}$	1.90	24.60	6.62±1.05	0.120±0.004
$70_V20_C10_{A1050}$	1.98	27.70	15.27±0.70	0.094±0.031
$70_V20_C10_{A1100}$	1.60	36.51	-	-
$80_{Vfl}20_{C950}$	1.98	25.40	18.48±1.18	0.074±0.072
$80_{Vfl}20_{C1000}$	2.04	17.74	-	-
$80_{Vfl}20_{C1050}$	2.15	17.34	-	-
$80_{Vfl}10_C10_{A950}$	1.70	32.54	-	-
$80_{Vfl}10_C10_{A1000}$	1.83	27.38	-	-
$80_{Vfl}10_C10_{A1050}$	1.53	39.28	16.51±4.36	0.026±0.003
$70_{Vfl}20_C10_{A950}$	1.89	25.00	-	-
$70_{Vfl}20_C10_{A1000}$	1.83	27.38	-	-
$70_{Vfl}20_C10_{A1050}$	1.42	39.28	-	-

Due to the poor densification process produced in bodies with Ar, the flexural strength decreases with the Ar addition but increases with the treatment temperature.

Despite the presence of porosity at higher temperature, these materials have sufficient strenght indicating an interesting potential for ArgAlum® recyling to produce new lightweight materials for bulding sector (Barbieri et al., 2013; Dondi et al., 1997).

4. Conclusions

This study has demonstrated the feasibility to use the glass wastes and a material from secondary aluminium scrap processing, in the manufacture of new green materials with composition different from ones of the traditional tiling ceramics, building bricks and roof tiles.

The possibility to obtain new ceramics, with higher waste concentration adopting a very short thermal cycle at relatively low temperatures of 950-1050°C was demonstrated. The results showed that, with the proper firing temperature, lightweight ceramic materials containing high amount of glass waste and a new product (ArgAlum®) can be produced. The low water absorption (< 1%), low density (< 2 g/cm^3) and the good flexural strength (16-20 MPa) were obtained with the addition of 10wt% of Argalum.

However, based on the results of the physical and mechanical properties, glass wastes and metallurgical industrial product are recommended as raw materials in the manufacture of ceramic products, reducing the amounts disposed in landfills, the consumption of raw materials and energy costs.

References

Alonso-Santurde R., Coz A., Viguri J.R, Andrés A., (2012), Recycling of foundry by-products in the ceramic industry: Green and core sand in clay bricks, *Construction and Building Materials*, **27**, 97-106.

Andreola F., Barbieri L., Lancellotti I., (2010), *End of Life-Materials: WEEE Glass Recovery in Construction Sector*, Second International Conference on Sustainable Construction Materials and Technologies, Università Politecnica delle Marche, Ancona, Italy.

Andreola F., Barbieri L., Giuranna D., Lancellotti I., Taurino R., (2013), Technical solutions to improve recovery of scraps derived from treating glass packaging waste, *Environmental Engineering and Managemnt Journal*, **12**, 57-60.

ArgAlum® PRODUCT INFORMATION data sheet: http://www.environdec.com/ec/Detail/epd580#.VVwnTJObWYe.

Barbieri L., Andreola F., Lancellotti I., Taurino R., (2013), Management of agricultural biomass wastes: Preliminary study on characterization and valorisation in clay matrix bricks, *Waste Management*, **33**, 2307-2315.

Candidate List of substances of very high concern for Authorisation: On line at: http://echa.europa.eu/web/guest/candiadate-list-table.

Co.Re.Ve., (2014), Part of the Specific Prevention Plan 2014 (Parte del Piano Specifico di Prevenzione 2014) Risultati di Raccolta e Riciclo 2013, On line at: http://www.reloaderitalia.it/documents/download/documenti_studi/2014/italia_del_riciclo_2014_schede_sintetiche.pdf.

Dondi M., Marsigli M., Fabbri B., (1997), Recycling of industrial and urban wastes in brick production, *Tile and Brick International*, **13**, 218–225.

EN 14411, (2006), Ceramic Tile Definitions, Classification, Characteristics and Marking, On line at: http://www.toetile.cn/UploadFiles/Others/20120103114502_15609.pdf.

Gastaldi P., Vedani V., (2008), Process and plant for the production of a solid component based on alumina from salt slag and white slag resulting from the fusion of secondary aluminium, (in Italian), Patent *No 000139194*, Italy.

Gil A., (2005), Management of the Salt Cake from Secondary Aluminium Fusion Processes, *Industrial & Engineering Chemistry Research*, **44**, 8852-885.

Gil A., Korili S.A., (2010), *Management of the Salt Cake Generated at Secondary Aluminium Melting Plants,* In: *Environmental Management*, Santosh Kumar, Sarkar Sciyo (Eds.), Croatia, 149-158, On line at: www.intechopen.com.

Jansma J.B., (2003), Fluorescent lamp coating recycling method Schenectady, Patent *No. 6531814,* New York, USA.

Johnston R.M., (1973), *Pigment handbook*, Patton T.C. (Ed.), John Wiley, New York, 229–288.

Li X.G., Lu Y., Ma B.G., Jian S., Tan H.B., Wu B., (2014), Utilization of oil well-derived drilling waste in shale-brick production, *Environmental Engineering and Managemnt Journal*, **13**, 173-180.

Manfredini T., Pellacani G.C., (1992), *Engineering Materials Handbook*, Vol 4, Ceramics and Glasses, ASTM, 925-929.

Szőke A.M., Munteain M., Dumitrascu O., Mészáros S., (2014), Studies on building ceramics manufacturing by incorporation dried sludge, *Environmental Engineering and Managemnt Journal*, **13**, 15-20

Tociu C., Diccu E., Maria C., (2014), Minimization of chemical risk by using recovered aluminum from metallurgical slag as coagulant in wastewater treatment, *Environmental Engineering and Managemnt Journal*, **13**, 429-434.

Tsakiridis P.E., (2012), Aluminium salt slag characterization and utilization-A review, *Journal of Hazardous Materials*, **217–218**, 1–10.

Watkins G., Husgafvel R., Paavola I.-L., (2013), Industrial residues – Is recycling now more straightforward?, *Waste Management*, **33**, 1-2.

Wöhlk W., Niederjaufner G., Hofmann G., (1987), *Recycling of Cover Salt in the Secondary Aluminium Industry*, In: *Crystallization and Precipitation,* 1st Edition Proceedings of the International Symposium, Strathdee G.L., Klein M.O., Melis L.A. (Eds.), Saskatoon, Saskatchewan, Canada, 99-108.